DELIVERABLES REPORT

MultiHemp

Multipurpose hemp for industrial bioproducts and biomass

(Ref n. 311849)

D5.6 Report on High-tech biobased composite applications.

February 2017

Carlos A. Fuentes

Aart W. Van Vuure

KU LEUVEN

1 MATERIALS AND METHODS

1.1 Materials

Hemp fibres were received from the Scuola di Dottorato per il Sistema Agroalimentare-Agrisystem (Italy). However, the fibres were harvested and scutched in Agritec (CZ), and then bio-degummed and hackled in Fibranova (Italy). Only fibres labelled as "H2" were considered for the production of composites at KU Leuven. The fibres were received in spiral-curled packs.

Two hemp accessions were selected for testing composite properties: FNPC 251 and FNPC-253. FNPC stands for the owner (Fédération Nationale des Producteurs de Chanvre), and the numbers are the codes of the accession. The nominal tensile strengths are 639.8±174.1 MPa and 782.6±164.4 MPa for FNPC-251 and FNPC-253 respectively (see report on fibre strength characterization, WP6).

Polyvinylidene fluoride (PVDF, Solef 1008) was used as the matrix phase. The polymer was obtained from Solvay as a film.

2.2 Composite preparation

The technique of the composite preparation is based on the techniques developed for bamboo fibre composites [1, 2]. Unidirectional composites were prepared by compression moulding of 4 or 5 stacks of prepregs consisting of aligned technical fibres, compressed between thermoplastic films.

A first step is to make pre-impregnated fibres (prepregs). These are made of one layer of extracted fibres and several layers of the selected polymer film (see Figure 1).

Figure 1 Aligned hemp fibres.

Fibres are aligned carefully on a plate covered with Teflon in sheets of at least 10 cm length and 5 cm width, since these are the dimensions of the final composite. These fibres are then fixated with tape and put in an oven at 60 °C for at least 3 days to dry thoroughly. The aligned fibres are shown in Figure 1.

After drying, some layers of the thermoplastic polymer are placed on top of and below the fibres. Then the fibres and polymer films are pressed at 180°C in order to prepare a tape of aligned fibres (prepreg). Prepregs were stored at 60°C to prevent problems due to moisture adsorption until composite manufacture.

In order to consolidate the sample and to prevent thermal degradation, a temperature of 200°C (25°C higher than the melting temperature of PVDF) and a pressure of 20 bars was used for only 5 minutes. This procedure aimed to ensure good impregnation. The fibre volume fraction was set at 40% by weight measurements. The density of technical fibres of hemp (1.56 g/cm^3) was measured in a gas pycnometer.

A sample of a composite obtained by the described procedure can be seen in Figure 2.

Figure 2 A10 cm x 5 cm x 0.3 cm hemp fibre composite.

2.3 Three point bending test

The flexural properties of hemp reinforced composites are evaluated by the three point bending test according to ASTM standard D790. The setup is shown in Figure 3.

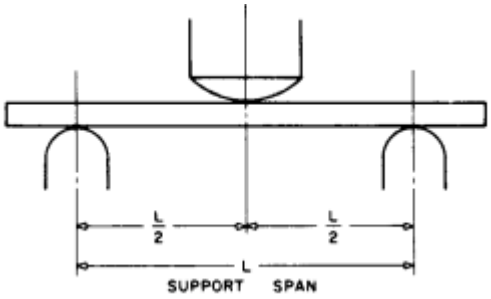

Figure 3 Three point bending test set up.

According to the standard test method, the modulus of elasticity in bending (Eb) can be calculated from equation 1:

$$E_b = \frac{L^3 m}{4bd^3} \qquad (1)$$

where Eb is the modulus of elasticity (MPa), L is the support span (mm), m is the slope of the tangent to the initial straight-line portion of the load-deflection curve (N/mm), b is the width of the sample (mm) and d is the thickness of the sample (mm).

The flexural stress (σf) can be calculated by equation 2:

$$\sigma_f = \frac{3PL}{2bd^2} \qquad (2)$$

where σf is the stress in the outer fibers at midpoint (MPa) and P is the load (N).

The flexural strain (ε_f) can be calculated using the equation 3

$$\varepsilon_f = \frac{6Dd}{L^2} \qquad (3)$$

where ε_f is the strain in the outer surface and D is the maximum deflection at the center of the beam (mm).

Flexural three point bending tests were performed on a universal testing machine (Instron 4426) in longitudinal and transversal direction to evaluate composite strength and interface strength respectively. The final dimensions of the samples were 50mm x 12mm x 3mm.

2.4 Strain mapping

A random speckle pattern was created on one side of the 3PBT samples (area equal to 12mm x 3mm) using an Airbrush Evolution from Harder & Steenbeck airbrush with a spray nozzle diameter of 0.15 mm (Harder & Steenbeck GmbH & Co. KG, Norderstedt, DE). A compressed air system provided a constant 2 bar pressure. Samples were prepared at 20° C and 50% RH.

In order to evaluate the quality of the speckle pattern, two methods were applied: pixel intensity histogram and strain deviation analysis [3, 4].

a) Pixel intensity histogram: The speckle pattern is qualitatively characterized by the image intensity histogram, where the amounts of pixels of a specific intensity are plotted. In this way the speckle distribution can be examined. The histogram is made in 8bit grayscale images with intensity values ranging from 0 to 255. According to Berfield et al. [3], acceptable speckle patterns

produce a Gaussian or bell-shaped distribution, while patterns not suitable for image correlation form two or more dominant peaks on both ends of the grayscale spectrum.

The image analysis was performed by using ImageJ 1.51g software (threshold function) (Wayne Rasband, National Institutes of Health, USA), which is also able to provide precise data regarding the number and size distribution of the speckles within the selected region of interest, thus providing also a quantitative characterization of the speckle pattern.

b) Strain deviation analysis: This methodology provides a control to compare and exclude speckle patterns that are not appropriate for digital image correlation. This technique consists in applying a virtual and uniform deformation on the image with the speckle pattern. Since the magnitude of the deformation is controlled and uniform, a homogeneous strain mapping over the entire image is expected. However, in reality digital resizing is not totally uniform, and local variations could be created depending on the method used for interpolation. The magnitude of these local variations of strain in uniformly deformed images, are related to imperfectly-speckled areas [4]. Then, the quality of a speckle pattern can be evaluated by comparing strain deviations along a horizontal arbitrarily chosen straight line over the image length. The virtual deformation was applied by using the lanczos3 resizing algorithm GIMP 2.8.1 software (GNU Image Manipulation Program, www.gimp.org).

2.5 Tomography

A Phoenix NanoTom X-ray computed tomography equipment (General Electric Company, Fairfield, USA) was used for scanning the sample before and after 3 point bending tests. The applied voltage and current were 53 kV and 245 µA respectively. The exposure time was 500 ms, and a frame averaging of 3 with an image skip of 1 was applied. The obtained voxel size was 6.47 µm.

For image processing and analysis, the 2D/3D image analysis software CTAn (v.1.16) (Bruker microCT, Kontich, BE) was used. Finally CTVol (v.2.3) software (Bruker microCT, Kontich, BE) was used for 3D space visualization.

3 RESULTS AND DISCUSSION

Table 1 shows the longitudinal and transversal properties of unidirectional PVDF hemp fibre composites, as well as the efficiency factors. The efficiency factor is the ratio of experimental longitudinal strength and the calculated value by following the rule of mixtures (the theoretical strength, see Figure 4). This factor is related to the effectiveness of load transfer between the polymer and the fibre, and it was calculated by considering a tensile strength of 639 MPa and 782.6 MPa for FNPC-251 and FNPC-253 respectively (4 specimens per accession were tested).

	FNPC-251			FNPC-253		
	Longitudinal		Transversal	Longitudinal		Transversal
	E-modulus (GPa)	Strength (MPa)	Strength (MPa)	E-modulus (GPa)	Strength (MPa)	Strength (MPa)
	16.8	239.8	17.8	17.8	182.7	14.4
Standard deviation	1.4	4.6	2.7	3.8	45.4	5.8
Efficiency Factor (%)	123.5	90.1		130.8	56.5	

Table 1 Three point bending test results (longitudinal and transversal directions).

The results for FNPC-251 specimens show an efficiency factor higher than 100% for the longitudinal Young's modulus value. This might indicate that elementary fibres are loaded rather than the technical fibres, since the back calculated E-modulus delivers Young's modulus values higher than those reported for technical fibres. This leads to the hypothesis that the technical fibres are suffering from partially detached elementary fibres, likely due to extraction damage. In the composite the elementary fibres can act on their own, when wetted well by the polymer matrix.

The longitudinal strength reached 90% of the theoretical value, which is high for a natural fibre thermoplastic composite. For instance, bamboo-PVDF and coir-PVDF composites reached

70% and 68% of efficiency respectively [5, 6]. The strength values obtained in this study are higher than those reported in literature for flax-polypropylene composites (~180MPa) [7] for the same volume fraction.

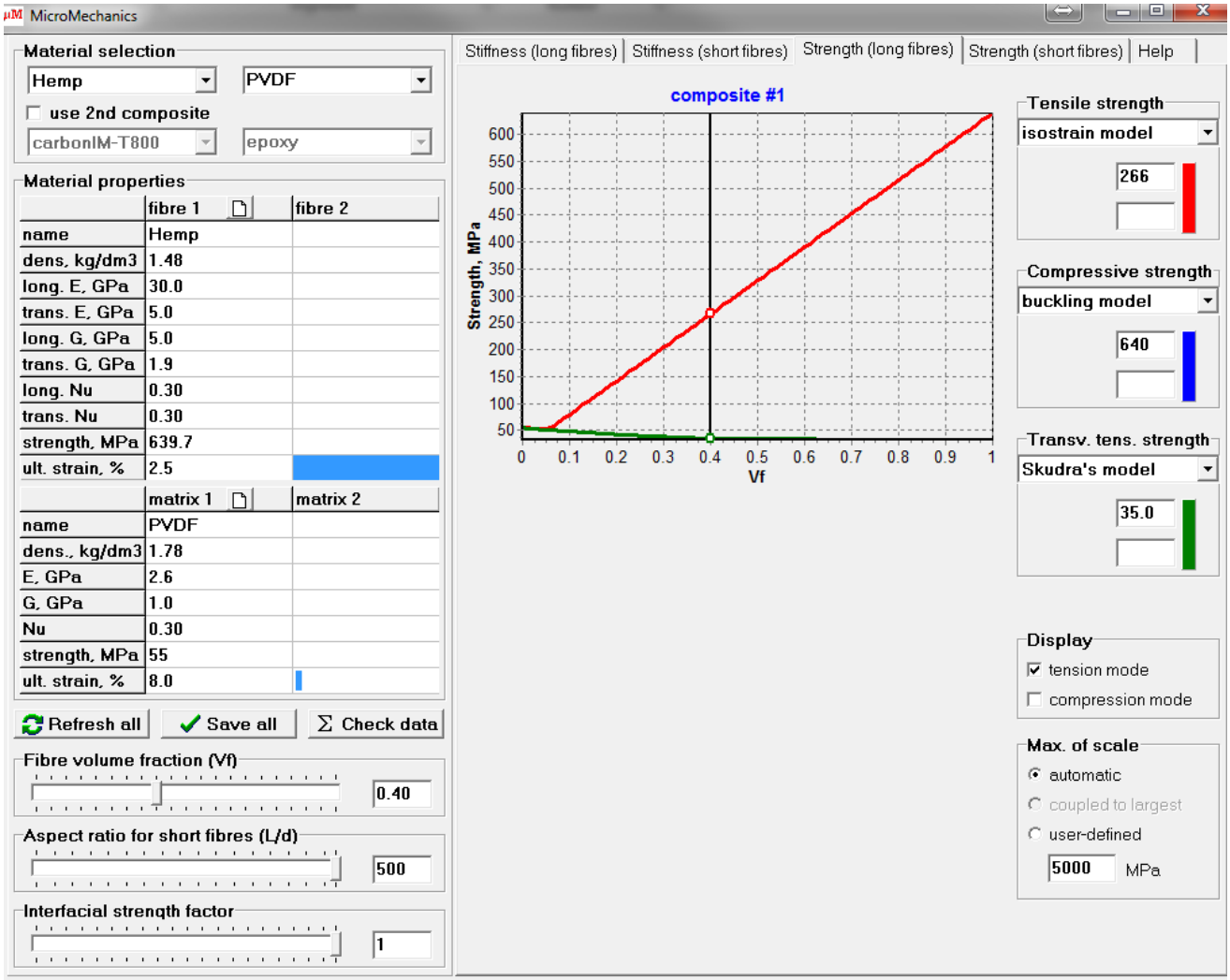

Figure 4 Calculation of the theoretical strength and Young's Modulus using the Micromechanics software for the accession FNPC-251.

In the case of FNPC-253, the efficiency factor is also higher than 100% for the Young's modulus value (see Figure 5). As in the case of FNPC-251, elementary fibres are likely loaded, since the back calculated E-modulus delivers Young's modulus values higher than those reported

for technical fibres. However, as it can be seen in Figure 5, the Young's modulus reached a maximum value around 1% of strain, and then dropped until zero. Also, the strength values were low, reaching only 56% of the strength theoretical value. This was not the case for the FNPC-251 material.

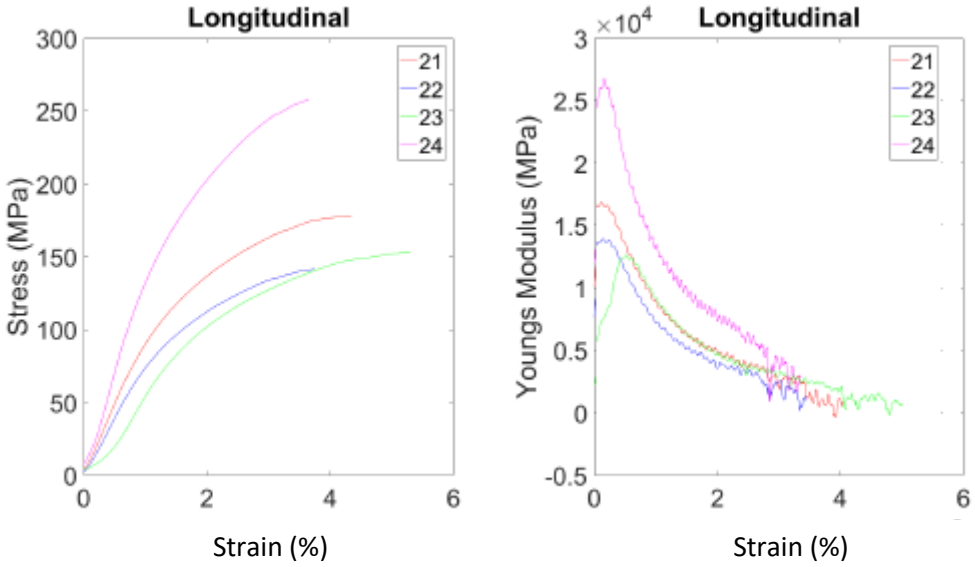

Figure 5 Stress-strain and Young's modulus-strain curves for the accession FNPC-253.

The behaviour of the FNPC-253 specimens might be explained by the effect of a delamination mechanism. Figure 6 presents the strain maps of a FNPC-253 specimen under flexion, where the global strain in the fibre direction, εxx, is increasing progressively and corresponds to 25%, 50% and 75% of the strain to failure value, and the moment just before failure of the composite. The maps show strain concentrations (tension and compression) in different zones, which indicates a complex mechanical behaviour. If shear strain is analysed (see Figure 7), it is clear that the composite is affected by development of shear strain between fibre layers (likely the original prepreg layers). It seems that a good consolidation between the different fibre layers was not achieved, although an overall good impregnation at the laminate level was obtained since the Young's modulus was high at low strain, as discussed in the previous paragraph. Tomography

analysis gives more evidence of delamination, as it can be seen in Figure 7, where an empty space along the bottom and parallel to the border of the sample can be observed.

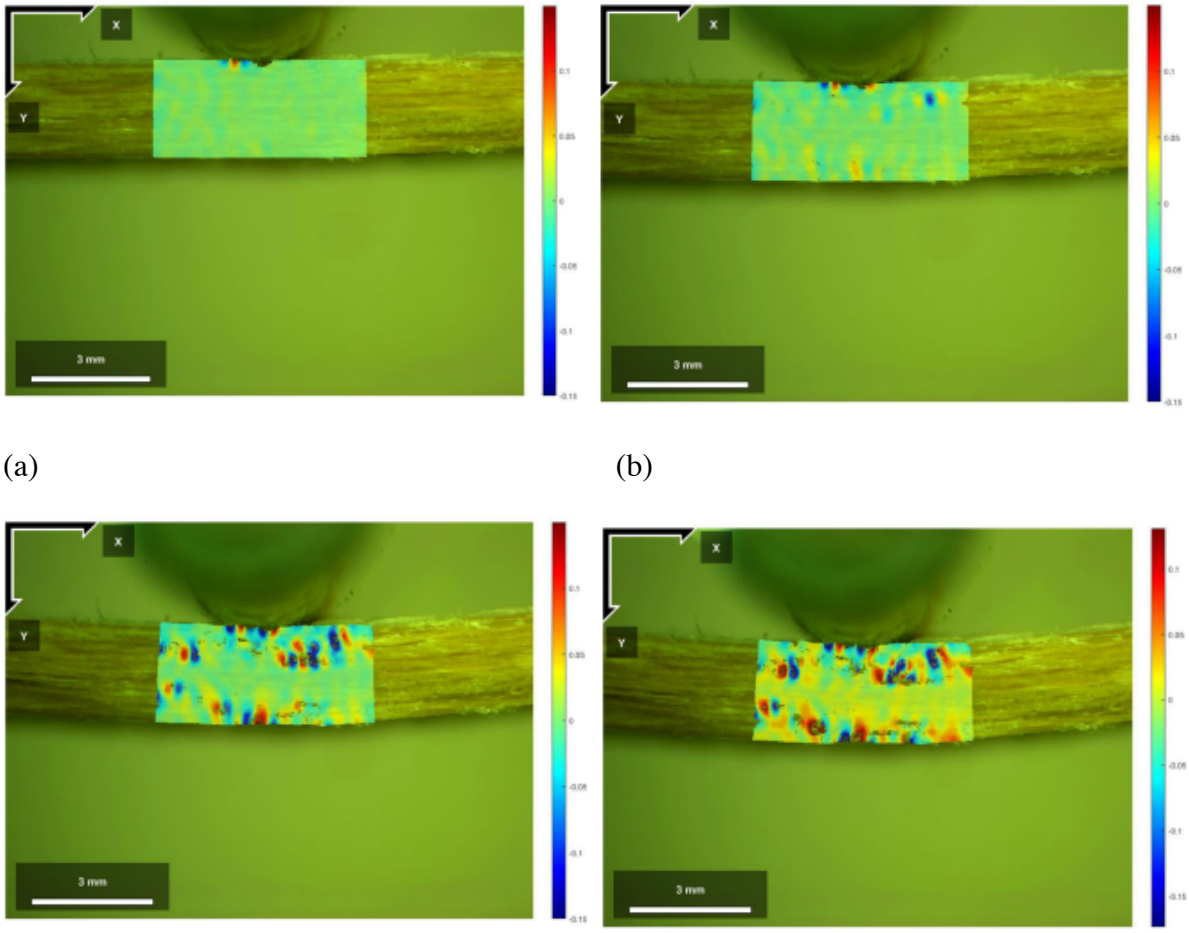

Figure 6 Full-field strain analysis in the fibre direction of a FNPC-253 specimen. Strain maps represent the gradual evolution of local strain at 3 levels of global strain (25%, 50%, and 75% of the strain to failure) and the local strain distribution an instant before failure.

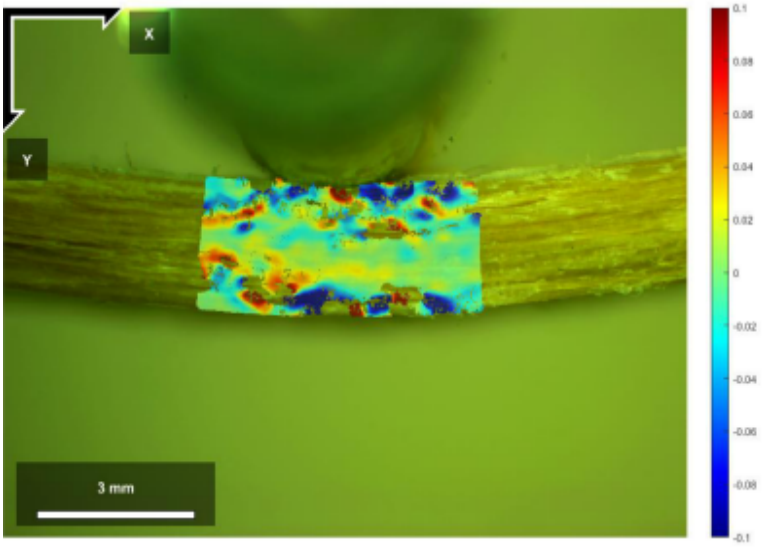

(a)

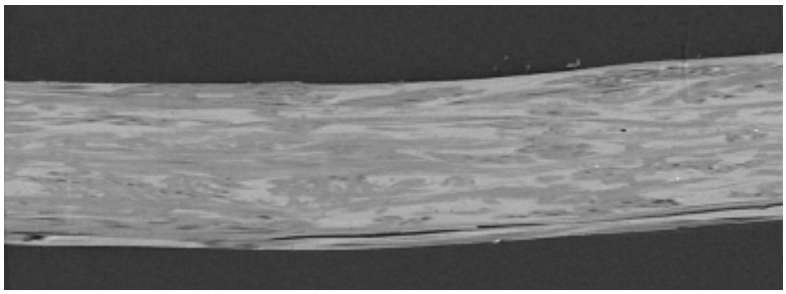

(b)

Figure 7 Full-field shear strain analysis of a FNPC-253 specimen, local strain distribution an instant before failure (a). Tomography image of a FNPC-253 sample after breakage (b).

The transverse 3-point bending test provides a direct estimation of interfacial tensile strength and practical adhesion if the fibre volume fraction is high enough (otherwise the matrix has a great influence). For this study the fibre volume fraction was set at 40%. The interfacial strength is reasonable to good for both accessions (17.8MPa and 14.4MPa for FNPC-251 and FNPC-253 respectively), comparable to those reported for bamboo-PVDF (23MPa) [6], coir-PVDF (17MPa) [8], and flax-PLA (19MPa) [9]. But the somewhat lower value for FNPC-253 perhaps indicates that the composite consolidation or fibre-matrix adhesion strength was somewhat less good for the FNPC-253 material; this may have triggered the loss in mechanical performance at higher strains.

4 FUTURE WORK

Hemp reinforced composites with thermoset matrices will be manufactured in order to further study the hypothesis that elementary fibres are loaded during deformation of the composite. A less viscous polymer can better impregnate the technical fibre, improving the load transfer from the matrix to the elementary fibre. Also, a detailed investigation of the interphase strength and its mechanism of failure by using in-situ tomography will be performed.

5 CONCLUSIONS

The strength of a hemp fibre reinforced thermoplastic composite can reach values close to the theoretical one (91% efficiency factor) with the appropriate processing conditions and parameters. The strength values are comparable to those reported for bamboo and flax thermoplastic composites, showing that hemp-based composites have a real potential as environmentally friendly materials in some applications (eg. Transport).

A substantial improvement of the Young's modulus can be observed at the composite level if compared with the values obtained for a technical fibre. This indicates the technical fibres show partial debonding of the elementary fibres after extraction; these can be reconnected by the matrix inside a composite.

REFERENCES

[1] L. Osorio, E. Trujillo, A. Van Vuure, I. Verpoest, Morphological aspects and mechanical properties of single bamboo fibers and flexural characterization of bamboo/epoxy composites, Journal of Reinforced Plastics and Composites 30(5) (2011) 396-408.
[2] E. Trujillo, M. Moesen, L. Osorio, A. Van Vuure, J. Ivens, I. Verpoest, Bamboo fibres for reinforcement in composite materials: Strength Weibull analysis, Composites Part A: Applied Science and Manufacturing 61 115-125.
[3] T. Berfield, J. Patel, R. Shimmin, P. Braun, J. Lambros, N. Sottos, Micro-and nanoscale deformation measurement of surface and internal planes via digital image correlation, Experimental Mechanics 47(1) (2007) 51-62.
[4] M. Mehdikhani, M. Aravand, B. Sabuncuoglu, M.G. Callens, S.V. Lomov, L. Gorbatikh, Full-field strain measurements at the micro-scale in fiber-reinforced composites using digital image correlation, Composite Structures 140 (2016) 192-201.
[5] C.A. Fuentes, L.Q.N. Tran, C. Dupont-Gillain, A. Van Vuure, I. Verpoest, Interfaces in Natural Fibre Composites: Effect of Surface Energy and Physical Adhesion, Journal of Biobased Materials and Bioenergy 6(4) (2012) 456-462.
[6] C.A. Fuentes, L.Q.N. Tran, M. Van Hellemont, V. Janssens, C. Dupont-Gillain, A.W. Van Vuure, I. Verpoest, Effect of physical adhesion on mechanical behaviour of bamboo fibre reinforced thermoplastic composites, Colloids and Surfaces A: Physicochemical and Engineering Aspects 418 (2012) 7-15.
[7] K. Van de Velde, P. Kiekens, Effect of material and process parameters on the mechanical properties of unidirectional and multidirectional flax/polypropylene composites, Composite Structures 62(3–4) (2003) 443-448.
[8] L.Q.N. Tran, C.A. Fuentes, C. Dupont-Gillain, A. Van Vuure, I. Verpoest, Understanding the interfacial compatibility and adhesion of natural coir fibre thermoplastic composites, Composites Science and Technology 80 (2013) 23-30.
[9] L. Tran, X. Yuan, D. Bhattacharyya, C. Fuentes, A. Van Vuure, I. Verpoest, Fiber-matrix interfacial adhesion in natural fiber composites, International Journal of Modern Physics B 29(10n11) (2015) 1540018.